Zootaxa 5717 (3): 383–402
https://www.mapress.com/zt/

Article

ISSN 1175-5326 (print edition)
ZOOTAXA
ISSN 1175-5334 (online edition)

https://doi.org/10.11646/zootaxa.5717.3.5
http://zoobank.org/urn:lsid:zoobank.org:pub:DC6BAA01-2859-4A81-8134-C1B853B5545C

A new microhylid frog species of the genus *Platypelis* from phytotelmata of *Pandanus* screw pines in the Sorata massif, northeastern Madagascar

ANDOLALAO RAKOTOARISON[1,2], ALICE PETZOLD[3], MARK D. SCHERZ[4], ANGELICA CROTTINI[5], JÖRN KÖHLER[6], OLIVER HAWLITSCHEK[7], FANOMEZANA M. RATSOAVINA[8], FRANK GLAW[9] & MIGUEL VENCES[10*]
[1]*Mention Environnement, Université de l'Itasy, Faliarivo Ambohidanerana, 118 Soavinandriana Itasy, Madagascar*
[2]*School for International Training, VN 41A Bis Ambohitsoa, 101 Antananarivo, Madagascar*
andomailaka@gmail.com; *https://orcid.org/0000-0003-2620-440X*
[3]*Institut für Biochemie und Biologie, Universität Potsdam, Karl-Liebknecht-Str. 24–25, 14476 Potsdam, Germany*
petzoldalice@gmail.com; *https://orcid.org/0000-0002-0743-2004*
[4]*Natural History Museum Denmark, University of Copenhagen, Universitetsparken 15, 2100 Copenhagen Ø, Denmark*
mark.scherz@gmail.com; *https://orcid.org/0000-0002-4613-7761*
[5]*Department of Biology, University of Florence, Via Madonna del Piano 6, I-50019 Sesto Fiorentino, Italy*
angelica.crottini@unifi.it: *https://orcid.org/0000-0002-8505-3050*
[6]*Hessisches Landesmuseum Darmstadt, Friedensplatz 1, 64283 Darmstadt, Germany*
joern.koehler@hlmd.de; *https://orcid.org/0000-0002-5250-2542*
[7]*Department of Evolutionary Biology and Environmental Studies, Universität Zürich, Winterthurer Str. 190, 8057 Zürich, Switzerland*
oliver.hawlitschek@uzh.ch; *https://orcid.org/0000-0001-8010-4157*
[8]*Mention Zoologie et Biodiversité Animale, Université d'Antananarivo, BP 906, Antananarivo, 101 Madagascar*
fanomezanarts@gmail.com; *https://orcid.org/0000-0003-1661-1669*
[9]*Zoologische Staatssammlung München (ZSM-SNSB), Münchhausenstr. 21, 81247 München, Germany*
glaw@snsb.de; *https://orcid.org/0000-0003-4072-8111*
[10]*Zoologisches Institut, Technische Universität Braunschweig, Mendelssohnstr. 4, 38106 Braunschweig, Germany*
m.vences@tu-braunschweig.de; *https://orcid.org/0000-0003-0747-0817*
**Corresponding author*

Abstract

We revise the molecular variation and taxonomy of an assemblage of lineages of endemic Malagasy cophyline microhylid frogs, previously considered to be allied to *Platypelis tetra.* Based on DNA sequences obtained from the *P. tetra* holotype via a museomics approach and further complementary DNA sequences of other specimens obtained by Sanger sequencing, we genetically characterize the species and reveal at least two additional genetic lineages associated to it. These differ by uncorrected pairwise distances of 4.4–5.0% in a fragment of the mitochondrial 16S rRNA gene and require taxonomic revision in future work. A further lineage previously assigned to *P. tetra* differs by 16S distances of 7.1–7.8% and occupies an isolated phylogenetic position. We here formally name and describe this new species from the Sorata Massif as *Platypelis efatra* **sp. nov.** and thereby increase the number of nominal *Platypelis* species to 18. We provide a description of its skeleton based on a micro-computed tomography scan of a paratype, which is the first detailed osteological description of a *Platypelis* species, and identify some possibly diagnostic osteological differences compared to *P. tetra*. We furthermore provide an updated advertisement call description for *P. tetra* from its type locality and briefly discuss the status of a divergent population from Ambodivoangy that we tentatively assign to *P. tetra* pending future study.

Key words: Amphibia; Anura; Cophylinae; *Platypelis*; integrative taxonomy, museomics, micro-CT, osteology

Introduction

The arboreal microhylid frogs of the genus *Platypelis* Boulenger have been the subject of substantial taxonomic research during the past few decades. The genus currently comprises 17 nominal species, of which more than half (nine species) were discovered and/or described after 2000 (Frost 2025). In addition, various candidate species

Accepted by W. Conradie: 25 Sept. 2025; published: 6 Nov. 2025

have been identified and provisionally characterized with a numbering system, but still await taxonomic revision (Andreone *et al.* 2005; Wollenberg *et al.* 2008; Vieites *et al.* 2009; Perl *et al.* 2014; Scherz *et al.* 2016; Glaw *et al.* 2020; Carné & Vieites 2024). The generic allocation of these frogs also requires more work, as some authors have considered *Platypelis* as a junior synonym of *Cophyla* Boettger (e.g. Peloso *et al.* 2016, 2017) and the relationships among the various taxa in the *Cophyla/Platypelis* clade have not yet been fully resolved (e.g., Scherz *et al.* 2016, 2017a).

As part of the subfamily Cophylinae, a species-rich radiation of microhylid frogs endemic to Madagascar (Andreone *et al.* 2005; van der Meijden *et al.* 2007; Wollenberg *et al.* 2008; Scherz *et al.* 2016), *Platypelis* frogs exhibit several traits that are characteristic for the group. These include endotrophic tadpoles typically developing in phytotelmic environments such as water-filled leaf axils and tree holes, and advertisement calls that typically consist of single tonal notes repeated without substantial variation at regular intervals for long periods of time (Glaw & Vences 2007). Similar to other subclades in the Cophylinae, species richness of *Platypelis* is concentrated in northern Madagascar (as defined by Brown *et al.* 2016: an area north of a diagonal spanning from ca. 15.5°S on the east coast to ca. 15.0°S on the west coast), where several species appear to be microendemic to specific mountain ranges.

Platypelis tetra Andreone, Fenolio & Walvoord, is a poorly known frog originally described from Anjanaharibe Sud in northern Madagascar. Subsequent studies tentatively assigned several *Platypelis* populations to *P. tetra* based on external morphological resemblance, and provisionally referred to them as "*P.* cf. *tetra*" (Gehring *et al.* 2010), "*P.* sp. 1" (Peloso *et al.* 2016), "*P.* aff. *tetra*" (Rakotoarison *et al.* 2020), "*P.* sp. aff. *tetra* 1" and "*P.* sp. aff. *tetra* 2" (Rosa *et al.* 2014; Rakotoarison *et al.* 2023), or formally designated them as unconfirmed candidate species *P.* aff. *tetra* UCS "Antsiranana", *P.* aff. *tetra* UCS "Bealanana", *P.* aff. *tetra* UCS "Sorata", and *P. tetra* UCS "South" (Carné & Vieites 2024). A formal taxonomic revision of these genetic lineages was long hampered by a lack of sequences from the type material or topotypical material, and the identity of *P. tetra* has thus remained unclarified until Rakotoarison *et al.* (2023) published a small Sanger-sequenced stretch of mitochondrial DNA from a *P. tetra* paratype. Here, we complement this information with a re-analysis of bioacoustic data for *P. tetra*, DNA sequences of the *P. tetra* holotype obtained using a museomics approach, Sanger sequences of additional specimens, and osteological examination based on micro-computed tomography. Based on these data, we clarify the species' genetic identity and variation, and formally name and describe one new species from the Sorata Massif that was found to be phylogenetically unrelated to *P. tetra*, despite superficial morphological resemblance.

Material and Methods

Sampling and external morphology

Frogs were collected at night and during the day by following the calling of males and through opportunistic searches in bamboo forest. Specimens were euthanized in MS-222 solution, fixed in 90% ethanol and preserved in 70% ethanol. Vouchers were deposited in the Zoologische Staatssammlung München (ZSM) and in the amphibian collection of the Mention Zoologie et Biodiversité Animale of the University of Antananarivo (UADBA-A). FGZC refer to field numbers of F. Glaw. Additional acronyms used in the molecular tree (FAZC, PSG, RAX, THC, ZCMV) refer to field numbers of F. Andreone, P.S. Gehring, C.J. Raxworthy, T.R. Fulgence, and M. Vences, respectively. Measurements were taken to the nearest 0.1 mm by AR using digital calipers. The measurement scheme follows that used by Rakotoarison *et al.* (2012): snout–vent length (SVL), maximum head width (HW), tibia length (TIBL), hindlimb length (HIL), head length (HL), horizontal eye diameter (ED), eye–nostril distance (END), nostril–snout tip distance (NSD), nostril–nostril distance (NND), horizontal tympanum diameter (TD), hand length (HAL), foot length (FL), foot length including tarsus (FOTL), forelimb length (FORL). We also report the position of the tibiotarsal articulation when the hindlimb is adpressed along the body (RHL).

Molecular genetics

A molecular phylogeny was reconstructed from DNA sequences of two adjacent fragments of the mitochondrial 16S rRNA gene (here called 16S-5' and 16S-3' to refer to their position close to the 5' or 3' terminus of the gene), complementing data from previous studies (e.g., Andreone *et al.* 2005; Wollenberg *et al.* 2008; Glaw *et al.* 2012, 2020; Rakotoarison *et al.* 2012, 2015, 2019, 2020, 2023; Rosa *et al.* 2014; Scherz *et al.* 2019). Specifically, as much as possible, we selected for each known species or candidate species, one representative individual for which both fragments were available. For specimens previously assigned to *P. tetra* or to related candidate species, we included all available samples for at least one of the two fragments, but made sure that at least one individual with both fragments was also available for each major genetic sublineage.

New sequences generated in this study were obtained after extracting DNA from muscle tissue samples stored in 99% ethanol, which were taken from animals in the field after euthanasia prior to fixation. DNA was extracted using a salt extraction protocol (Bruford *et al.* 1992) and the two 16S fragments were PCR-amplified with the primers 16SL3 (AGCAAAGAHYWWACCTCGTACCTTTTGCAT) and 16SAH (ATGTTTTTGATAAACAGGCG) of Vences *et al.* (2003) for 16S-5', and 16Sar-L (CGCCTGTTTATCAAAAACAT) and 16SBr-H (CCGGTCTGAACTCAGATCACGT) of Palumbi *et al.* (1991) for 16S-3', with the following PCR protocols: for 16S-5' 90 s at 94 °C, followed by 33 cycles of 45 s at 94 °C, 45 s at 52 °C, 90 s at 72 °C, and a final extension step of 300 s at 72 °C; and for 16S-3' 90 s at 94 °C, followed by 33 cycles of 45 s at 94 °C, 45 s at 55 °C, 90 s at 72 °C, and a final extension step of 300 s at 72 °C. We purified PCR products with ExoSAPIt (Thermo Fisher Scientific, Waltham, MA, USA) and sent them for sequencing on an automated capillary DNA sequencer at LGC Genomics (Berlin, Germany) using the respective forward primers. The obtained chromatograms were checked by eye, and poor-quality terminal sections were trimmed with CodonCode Aligner 3.7.1 (Codon Code Corporation, Dedham, MA, USA). Newly obtained sequences were submitted to GenBank (accession numbers PX275628–PX275639). A table with all sequences, accession numbers, voucher numbers and sampling localities has been archived in the Zenodo repository (https://doi.org/ 10.5281/zenodo.17086824), along with alignments and tree files.

The holotype of *P. tetra* (MRSN A2174), housed at the Museo Regionale di Scienze Naturali of Torino, was loaned to the University of Potsdam, Germany, for the purpose of this study. Tissue was excised from the liver in a minimally-destructive manner with sterile scalpels and tweezers. The sample was then weighed and incubated in a Guanidine Thiocyanate (GuSCN) based extraction buffer solution at 37°C overnight. The next day, a total volume of ca. 25 µl genomic DNA was extracted following the protocol of Rohland *et al.* (2004), including several consecutive steps as described in Straube *et al.* (2021). The yield of DNA was quantified based on 1 µl DNA extract using the Qubit dsDNA HS Assay Kit 0.2–100 ng/µl (Life Technologies, Carlsbad, California, US) according to the manufacturer's instructions. A maximum of 13 ng DNA was used as input for single-stranded library preparation following the protocol of Gansauge *et al.* (2017). All lab work prior to qPCR was conducted in a dedicated DNA facility at the University of Potsdam, Germany, which meets all requirements to work with historical samples (see Fulton & Shapiro 2019) and extraction and library blanks were run alongside all samples to check for contamination. Final library concentrations and fragment length distributions were assessed using a 2200 TapeStation (Aligent Technologies) assay. Sequence data was obtained through shotgun-sequencing of approximately one million 75 bp single-end reads using an Illumina Nextseq 500/550 sequencing platform at the University of Potsdam, following the procedure described in Paijmans *et al.* (2017). The quality of the obtained reads was visualized twice using FastQC (https://www.bioinformatics.babraham.ac.uk), both before and after trimming of Illumina adapter sequences and discarding reads shorter than 30 bp with cutadapt v1.12 (Martin 2011). Mapping of reads was performed in Geneious Prime v.2022.0.1 (Biomatters Ltd., Auckland, New Zealand) using a consensus sequence of 16S for the genus as a reference, which was derived from an alignment including sequences from all currently recognized *Platypelis* species that were publicly available on GenBank. Individual mapping was run for 100 iterations using a mapping quality filter of 30 and medium-low sensitivity options. The obtained contigs were assembled into a consensus sequence of 16S with missing sections in-between contigs coded by the letter "N".

We used Concatenator (Vences *et al.* 2022), which is part of the iTaxoTools software package (Vences *et al.* 2021), to separately align the two 16S fragments using the G-INS-I algorithm of MAFFT (Katoh & Standley 2013), and subsequently concatenate them. We used MEGA 7 (Kumar *et al.* 2016) to select the best-fitting substitution model (GTR+G) for the concatenated data based on the Bayesian Information Criterion and ran a phylogenetic analysis under the Maximum Likelihood (ML) optimality criterion in RAxML (Stamatakis 2014) as implemented in raxmlgui (Edler *et al.* 2021), with 500 thorough bootstrap replicates to assess node support. Based on previous multi-gene analyses (Scherz *et al.* 2016) we used *Cophyla* as outgroup and rooted the tree at the *Cophyla/Platypelis* node.

Uncorrected pairwise divergences were calculated in MEGA 7 from the MAFFT-aligned sequences of the 16S-3' fragment which has been more commonly used in previous molecular taxonomic assessments and genetic distance comparisons in Malagasy frogs (e.g., Vieites *et al.* 2009).

Bioacoustics

Vocalizations of *P. tetra* at Ambodivoangy were recorded in the field using a Tascam DR-07 digital recorder with built-in microphones at 44.1 KHz and 16-bit resolution and saved as uncompressed waveform audio file format (.wav). The call recording of *P. tetra* from its type locality (sound file published by Vences *et al.* 2006: CD3, track 61), used by Andreone *et al.* (2003) in the species' original description, was re-analyzed herein because the numerical call parameters for this recording provided by Andreone *et al.* (2003) were partly in error. Recordings were re-sampled at 22.05 kHz and 32-bit resolution and computer-analyzed using the software Cool Edit Pro 2.0. We obtained frequency information through Fast Fourier Transformation (FFT; width 1024 points) at Hanning window function. Spectrograms were produced with Blackman window function at 256 bands resolution. Sensitive filtering was applied to remove background sounds, applied only to frequencies outside the prevalent bandwidths of calls. Temporal measurements are summarized as mean ± standard deviation with range in parentheses. Description and terminology follow Köhler *et al.* (2017), using the call-centered terminological scheme.

Osteology

Micro-computed tomography (micro-CT) scans of two specimens (ZSM 1621/2012 and ZSM 42/2011) were produced on a nanotom m nano-CT scanner (GE Measurement & Control, Wunstorf, Germany) at the Zoologische Staatssammlung München, Munich, Germany, with a molybdenum target and a 0.1 mm copper filter at a voltage of 140 kV and current of 80 µA, with a timing of 750 ms for 2440 projections, and reconstructed into 3D volumes in datos|x reconstruct (GE Measurement & Control, Wunstorf, Germany); and that of the holotype of *P. tetra*, MRSN A2174, was produced on a Nikon XT H 225ST (Nikon Corp., Tokyo, Japan) at the Danish Technical University, Copenhagen, Denmark with a Wolfram target and without a filter, at a voltage of 80 kV and a current of 250 µA (20 W), with a timing of 700 ms for 3241 projections (voxel size 20.284 µm) and reconstructed into 3D volumes with the Nikon reconstruction package. Both were converted into unsigned 8-bit volumes and visualized in VG Studio Max (Volume Graphics GMBH, Heidelberg, Germany). Osteological descriptions are based on screenshots produced in VG Studio Max, following recommendations of Scherz *et al.* (2017b). Osteological terminology follows Scherz *et al.* (2017b), which is based on Trueb (1968, 1973) and Fabrezi & Alberch (1996). Scans are available from https://www.morphosource.org/projects/000790016.

Results

The concatenated alignment of the two 16S fragments consisted of 1163 base pairs (nucleotides), of which 649 bp corresponded to the 16S-5' fragment and 514 to the 16S-3' fragment. The ML tree inferred from this dataset (Fig. 1) agreed with previously published phylogenetic reconstructions that were mainly based on the same sequences for most species (e.g., Rakotoarison *et al.* 2023). In general, the relationships were relatively poorly supported at deep nodes. However, three main clades (here named P1–P3) within *Platypelis* received bootstrap support (BS) >70%: clade P1 (BS = 76%) containing *P. ando, P. barbouri, P. karenae, P. milloti, P. pollicaris, P. ranjomena, P. ravus, P. tetra*, and *P. tuberifera*, candidate species *P*. sp. Ca09 and *P*. sp. Ca01, and the focal lineage from Sorata; clade P2 (BS = 77%) contains a set of species mainly distributed in mountain massifs of northern Madagascar, i.e., *P. alticola, P. laetus, P. mavomavo, P. olgae, P. saikamavo,* and *P. tsaratananaensis* and candidate species *P*. sp. Ca12 and *P*. sp. Ca13; and clade P3 (BS = 99%), only containing *P. grandis*. The relationships between these three main clades (P1–P3) remain unsupported.

The focal lineage from Sorata was not resolved as closely related to *P. tetra*, but instead split from the basalmost node in clade P1, being sister to a monophyletic group of all other species in clade P1 (BS = 70%). Within *P. tetra*, several deep sublineages were observed corresponding to samples from (i) Ambodivoangy, Makira, Farankaraina, and Ambodiriana, (ii) Makira and Anjanaharibe-Sud, and (iii) Antalaha region and Marojejy East (see map in Fig. 2). The *P. tetra* paratype (MRSN A2165) was represented by a 360 bp sequence of only the 16S-3' sequence, whereas the *P. tetra* holotype had 196 bp and 224 bp (interrupted by stretches of missing data) for the 16S-5' and 16S-3' fragments, respectively. The long branch of the *P. tetra* paratype and its unclarified placement in the tree may have been caused by sequencing errors or an uneven distribution of the available data for it (only one of the two 16S fragments), whereas the *P. tetra* holotype sequences clustered with a *P. tetra* sample from Makira (FGZC 5674). The focal lineage from Sorata was sister to two other samples from Andramanalana and Lohandroranga.

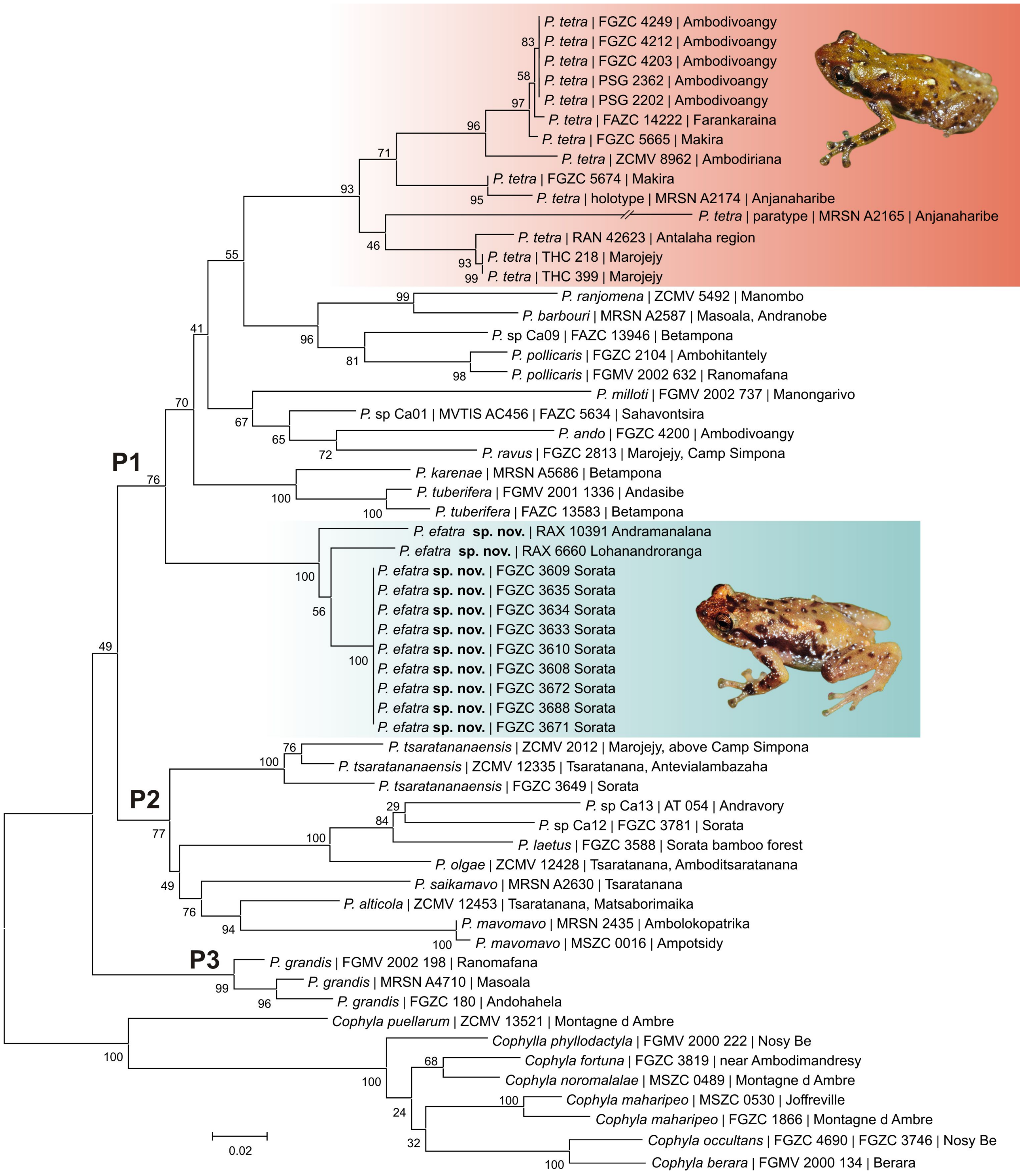

FIGURE 1. Maximum likelihood tree inferred from DNA sequences (1163 bp) of two fragments of the mitochondrial 16S rRNA gene for species of *Platypelis*. Numbers at nodes are bootstrap proportions in percent (500 replicates). The tree was rooted with *Cophyla* as outgroup. P1–P3 refer to major clades within *Platypelis* as described in the text. The paratype of *P. tetra* (MRSN A2165) had a very long branch likely caused by its many missing data (shortened in the tree for better graphical representation). Image of the holotype of *P. efatra* **sp. nov.** (ZSM 1621/2012) mirrored to match the orientation of the holotype of *P. tetra* (MRSN A2174).

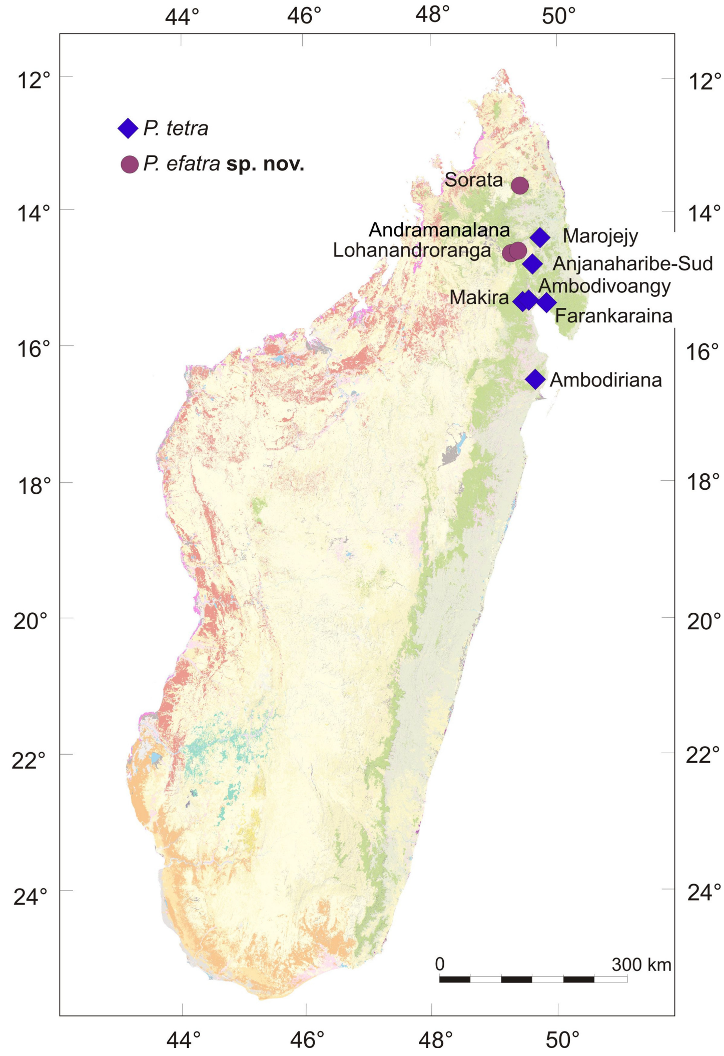

FIGURE 2. Distribution map showing genetically confirmed records of *Platypelis efatra* **sp. nov.** and of specimens assigned to *P. tetra.* The base map shows vegetation across Madagascar from the Madagascar Vegetation Mapping Project, available at https://web.archive.org/web/20180419112513/http://www.vegmad.org/). Vegetation is colored as follows: green, humid forest (rainforest); red, western dry deciduous forest; pink, mangroves; orange, spiny forest-thicket; greenish blue, western subhumid forest; yellow, Tapia forest.

Uncorrected pairwise distances calculated from the 16S-3' sequences amounted to 6.2–11.1% between *P. tetra* and other nominal *Platypelis* species, 5.4–9.4% between the focal lineage from Sorata and other nominal *Platypelis* species, and 7.1–7.8% between the Sorata lineage and *P. tetra*. Distances between the main sublineages of *P. tetra* ranged between 4.4–5.0%.

Morphologically we observed only a limited amount of differentiation between topotypical *P. tetra* and the Sorata lineage, mostly a weaker expression of the four symmetrical dorsal tubercles and a possibly stronger expression of the canthus rostralis in the Sorata lineage (Figs 3–4; Diagnosis below). A set of further possible differences was found in osteology (reported in the osteological comparison below) but rely on data for just one individual of the new species. However, the very high genetic divergence (much higher than the amounts that so far have been observed between conspecific populations of frogs; e.g., Vieites *et al.* 2009) and its isolated phylogenetic position strongly suggest a differentiation of the Sorata lineage at the level of a distinct species, and it is therefore formally named and described in the following section.

FIGURE 3. Images of individuals in life assigned to *Platypelis tetra*. A, holotype MRSN A2174 from Analabe valley, Anjanaharibe-Sud; B, C, ZSM 409/2010 (FGZC 4212) from Ambodivoangy. D and E, two additional specimens from Ambodivoangy (photos not clearly assignable to a voucher specimen).

***Platypelis efatra* sp. nov.**

Figures 4–5

Remark. Based on DNA sequences, this species has previously been referred to under the names *P. tetra* by Rosa *et al.* (2014), *P.* aff. *tetra* by Rakotoarison *et al.* (2020) and *P.* aff. *tetra* UCS "Sorata" by Carné & Vieites (2024).

Holotype. ZSM 1621/2012 (FGZC 3609), adult female with mature oocytes, collected on 26 November 2012, in the Sorata Massif (near 13.6817°S, 49.4411°E, 1339 m a.s.l.), now included in the protected area COMATSA Nord, northern Madagascar, by F. Glaw, O. Hawlitschek, T. Rajoafiarison, A. Rakotoarison, F.M. Ratsoavina, and A. Razafimanantsoa.

Paratypes. Eight paratypes: ZSM 1619/2012 (FGZC 3671) and UADBA-FGZC 3672, two unsexed individuals collected on 28 November 2012, in the Sorata Massif (near 13.675°S, 49.4392°E, 1580 m a.s.l.) by the same collectors as the holotype; ZSM 1620/2012 (FGZC 3608), adult female with mature oocytes, and ZSM 1622/2012 (FGZC 3610), sex undetermined, with same collection data as the holotype; UADBA-FGZC 3633, UADBA-FGZC 3634 and UADBA-FGZC 3635, three unsexed individuals with same collection data as the holotype but collected on 27 November 2012; UADBA-FGZC 3688, a female, collected on 28 November 2012, in bamboo forest above the Sorata camp site by the same collectors as the holotype. The paratypes in the UADBA collection were not studied morphologically, but are genetically almost identical to the ZSM type specimens (see Fig. 1).

Definition. Assigned to the genus *Platypelis* in the microhylid subfamily Cophylinae based on occurrence in Madagascar, enlarged terminal discs on fingers and toes, absence of nuptial pads, absence of femoral glands, and molecular phylogenetic relationships. The species can be distinguished from other cophylines by the combination of the following character states: (1) medium-sized species (adult female SVL 21.2–22.1 mm); (2) manus with second finger slightly shorter than fourth; (3) pes with third toe slightly longer than fifth; (4) dorsum with four symmetrically arranged and distinctly enlarged white tubercles; (5) absence of red color on limbs and ventral side; (6) absence of distinct yellow color on posterior belly and ventral sides of hindlimbs; (7) absence of greenish color on the throat and the belly; (8) presence of a dark dorsolateral stripe running from the eye to a point behind the axilla or further.

Diagnosis. *Platypelis efatra* **sp. nov.** differs from most specimens of *Cophyla maharipeo*, *C. noromalalae* and *C. puellarum* by smaller body size (SVL 19.4–22.1 mm vs. SVL up to 33.7 mm); from *C. fortuna, C. occultans* and *C. phyllodactyla* by having the third toe longer than fifth (vs. third toe slightly shorter than fifth); from *C. berara* by having the third toe longer than fifth (vs. both toes of similar length). Within *Platypelis*, the new species can be distinguished by a set of morphological characters from all congeners, of which we here highlight the most important characters. *Platypelis efatra* **sp. nov.** can be distinguished from all *Platypelis* species except for *P. tetra*, *P. tuberifera* and *P. karenae* by the presence of a dark band running from the eye to the forelimb insertion or beyond (vs. absence); from *P. grandis, P. alticola* and *P. tuberifera* by smaller body size (adult body size SVL 19.4–22.1 mm vs. 30–105 mm), and furthermore from *P. grandis* by largely smooth dorsal skin (vs. many large tubercles); from *P. karenae* by dorsal surface with dark markings and washed with irregular dark pigment (vs. typically uniformly yellowish light brown); from *P. tuberifera* and *P. cowanii* by smaller body size (adult SVL 19.4–22.1 mm vs. 30–40 mm); from *P. tsaratananaensis* and *P. pollicaris* by presence of four symmetrically arranged and distinctly enlarged white tubercles on dorsum (vs. absence); from *P. ravus* by presence of four symmetrically arranged and distinctly enlarged white tubercles on dorsum (vs. presence of moderately-sized tubercles); from *P. olgae* and from *P. laetus* by absence of greenish or green-yellow ventral color (vs. presence); from *P. ando* by the tibiotarsal articulation reaching between forelimb and tympanum when hindlimb adpressed along body (vs. reaching the tympanum); from *P. milloti* by absence of red ventral color and absence of distinct dorsal pattern of sharply delimited black markings and light vertebral stripe (vs. presence); from *P. barbouri* and *P. ranjomena* by absence of red color on ventral surfaces and limbs (vs. presence); from *P. saikamavo* by the absence of yellow coloration on the ventral side of belly and limbs (vs. presence); from *P. mavomavo* by absence of yellow color on belly (vs. presence in some populations) and smaller body size (adult SVL 19.4–22.1 mm vs. 21.8–32.3 mm).

Morphologically, the new species is most similar to *P. tetra* which, however, is phylogenetically not its closest relative. Due to a limited knowledge of the variation of *P. tetra* which may be a species complex, the following comparison is restricted to characteristics observed in the type material of *P. tetra* from Anjanaharibe Sud: the new species differs from these specimens according to data from Andreone *et al.* (2003), a photo probably corresponding to the holotype (Fig. 3A), and our own examination of paratype MRSN A2172 by less distinct expression of symmetrical dorsal tubercles (four to six symmetrical tubercles visible, but especially the anterior pairs smaller than in *P. tetra*), a distinct canthus rostralis (vs. possibly more indistinct), and possibly larger body size of females (up to 22.1 mm vs. up to 19.4 mm; Andreone *et al.* 2003). Osteologically, it differs most clearly by a well developed dorsal prominence and oblique groove on the iliac shafts (vs. indistinct), and more hatchet-shaped sacral diapophyses with an anteriorly angled anterior edge (vs. more triangular, with the anterior edge running perpendicular to the body axis). Several additional differences are present (see Comparative osteology section below), but their significance and consistency is difficult to assess without scans of more individuals per species.

Description of the holotype. Adult female, with mature oocytes visible through the ventral skin, in relatively good state of preservation (Fig. 5), some muscle tissue removed from left thigh; snout–vent length 21.2 mm (for further measurements see Table 1); body relatively plump; head slightly wider than long, not wider than body; snout slightly rounded in dorsal view, bluntly rounded in lateral view; nostrils not protuberant, nearer to tip of snout than to eye; canthus rostralis distinct, straight; loreal region straight, slightly oblique; tympanum distinct, 32.4% of eye diameter; supratympanic fold distinct, starting at posterior border of eye and ending anterior to forelimb; tongue long, broadening posteriorly, attached anteriorly, not notched; maxillary teeth present, vomerine teeth barely recognizable by superficial examination but present as two rudimentary aggregations posteriomedially to choanae; choanae rounded. Forelimbs robust; subarticular tubercles single, indistinct; outer metacarpal tubercle small, rounded; hand without webbing; terminal finger discs broadly rounded to slightly bilobate, with lateral fringes; relative length of fingers 1<2<4<3; nuptial pads absent. Hindlimbs slender; tibiotarsal articulation reaching between forelimb and tympanum when hindlimb adpressed along body; tibia length 47.6% of SVL; inner metatarsal tubercle small, oval; outer metatarsal tubercle absent; webbing between toes largely absent, limited to traces of webbing between third and fourth toe; subarticular tubercles on toes single; toes with flattened discs which are relatively broad and of slightly bilobate shape; relative length of toes 1<2<5<3<4; third toe slightly longer than fifth; skin dorsally smooth, without dorsolateral folds, with two distinctly enlarged and pointed symmetrical tubercles on the lower back and several smaller tubercles scattered on anterior back; ventral skin smooth.

After thirteen years in 70% ethanol, the dorsal surface is light brown, with dark brown markings distributed across the head, dorsum, and limbs. A distinct dark brown W-marking on the posterior dorsum, a dark X-marking on head and anterior dorsum. Additional elongated blotches and diffuse speckling are scattered across the dorsum, becoming denser along the flanks and dorsal surfaces of the thighs. Two symmetrically arranged distinct white tubercles are present on the posterior dorsum, several smaller white tubercles scattered on anterior back; symmetrical tubercles on anterior dorsum cannot be clearly recognized. The head is slightly darker than the rest of the dorsum, especially posterior to the eyes. A dark band runs from the eyes to almost reaching the forelimb insertion. Digits and toe tips are light brown, with dark brown color dorsally on hand, forearms, and thighs. The ventral surface is pale beige to yellowish cream.

In life (Fig. 4), similar to preservative but more contrasted. Some light color is visible dorsally, lining the dark W-shaped marking on the posterior dorsum and at the posterior edges of eyes. Two symetrically arranged white tubercles are also visible on the anterior dorsum (not clearly recognizable in preservative). The ventral side is uniformly gray-pinkish with a yellowish tint on the throat.

Variation. The examined paratypes agree well with the holotype in general morphology despite considerable individual variation in color pattern (Fig. 4). Paratype ZSM 1620/2012 (FGZC 3608) is a female with mature oocytes visible through the ventral skin, as in the holotype, and of similar body size as the holotype (Table 1). ZSM 1622/2012 (FGZC 3610) is distinctly smaller and might be a male, but the prepollex on its hand is not strongly developed and we could not assess sexual maturity; in life, this specimen had two distinct light beige rhomboid markings in the central dorsum, and a rather yellowish throat (Fig. 4)

Osteology. Based on a micro-CT scan of paratype ZSM 1620/2012 (Fig. 6). The skeleton shares key characteristics with other members of the genus *Platypelis* (given by Scherz *et al.* 2022): postchoanal and prechoanal vomer elements present; two small aggregations of vomerine teeth on the vomers, separated medially by a distinct gap; strongly curved clavicles starting near the midpoint of the coracoid; fingers and toes with Y-shaped distal phalanges. So far, no detailed description of the osteology of a *Platypelis* species has been published. We therefore provide such an account here:

Overall, the skeleton is well ossified, with all bones and bone endings clearly distinct. The skull is almost equilateral.

Dorsal investing bones. Nasals separated by a wide gap, without contact to any other bones, lachrymiform, with a very tapered and sharp maxillary process that does not approach the facial process of the maxilla. Frontoparietals well ossified, with a narrow gap separating them along the midline; in posterior contact with the exoccipital, lateral

TABLE 1. Morphometric measurements (all in mm) of specimens of *Platypelis efatra* **sp. nov.** and specimens assigned to *P. tetra*. Abbreviations: HT, holotype; PT, paratype, F, female; M, male. See materials and methods for abbreviations of measurements. To preserve characters for future morphological and anatomical study, specimens were not dissected, and the sex of several individuals is therefore in need of confirmation. Specimen marked with an asterisk (*) was not sequenced.

Catalog number	**Field number**	**Locality**	**Status**	**Sex**	**SVL**	**HW**	**HL**	**TD**	**ED**	**END**	**NSD**	**NND**	**FORL**	**HAL**	**HIL**	**FOTL**	**FOL**	**TIL**
P. efatra **sp. nov.**																		
ZSM 1620/2012	FGZC 3608	Sorata	PT	F	22.1	8.7	7.1	1.2	3.8	2.3	1.6	2.2	12.5	6.1	29.1	12.3	7.1	10.4
ZSM 1621/2012	FGZC 3609	Sorata	HT	F	21.2	7.6	6.1	1.2	3.7	2.1	1.1	2.4	12.1	6.2	27.1	12.4	8.1	10.1
ZSM 1622/2012	FGZC 3610	Sorata	PT	M?	17.1	7.1	5.1	1.1	2.2	1.6	1.1	2.7	11.8	4.2	23.3	11.2	5.1	9.6
ZSM 1619/2012	FGZC 3671	Sorata	PT	F?	19.4	6.5	6.5	1.2	3.5	2.1	1.1	2.1	11.9	5.9	25.6	12.1	7.2	9.7
P. tetra																		
MRSN A2172	NA	Anjanaharibe Sud	PT	F?	17.1	6.2	6.5	1.4	3.2	1.1	1.1	2.5	10.2	4.2	24.7	9.5	6.3	8.3
ZSM 168/2022	FGZC 5674	Makira		M?	17.1	5.1	6.1	1.4	3.1	1.2	1.1	2.5	9.8	3.2	20.2	9.7	5.9	8.1
ZSM 169/2022 *	FGZC 6546	Makira		M?	17.7	5.3	6.1	1.2	3.0	1.1	1.2	2.3	10.0	3.1	21.2	9.9	6.1	8.5
ZSM 409/2010	FGZC 4212	Ambodivoangy		M?	13.1	5.7	5.1	1.1	2.4	1.1	1.2	1.4	8.1	3.2	20.0	9.1	4.2	7.2
ZSM 410/2010	FGZC 4249	Ambodivoangy		M?	15.1	5.1	5.1	1.1	2.9	1.1	1.1	1.8	9.7	3.2	22.7	9.8	5.1	8.5

FIGURE 4. Images of individuals in life assigned to *Platypelis efatra* **sp. nov.**, all from Sorata. A, B, female paratype ZSM 1620/2012 (FGZC 3608); C, D, female holotype ZSM 1621/2012 (FGZC 3609); E, F, ZSM 1622/2012 (FGZC 3610).

FIGURE 5. Preserved holotype ZSM 1621/2012 (FGZC 3609) of *Platypelis efatra* **sp. nov.** from Sorata in dorsal (left) and ventral (right) views.

contact with the prootic, and anterolateral contact with the sphenethmoid. Dorsal surface smooth, without dorsal processes.

Neurocranium. Sphenethmoid ossified, forming a brace to the lateral anterior braincase between the frontoparietal above and parasphenoid cultriform process below, anteriorly extending beyond the tip of the cultriform process and ventrolaterally bracing the neopalatine.

Exoccipitals meeting only superficially dorsally and without contact posteriorly or ventrally, forming the fenestra ovale. Prootic substantially ossified; the prootic foramen (through which the trigeminal and other nerves pass) is not enclosed in this bone but presumably is closed anteriorly by the pila antotica. Septomaxilla curled, well ossified. Columella elongate, the pars interna plectri indented on its proximal surface, the anterodorsal surface continuous without substantial curve with the pars media plectri, the posteroventral surface distinctly set apart from the pars media plectri.

Ventral investing and palatal bones. Parasphenoid with broad and anteriorly subtly broadening cultriform process, short alary processes, and a bulbous posterior prominence that does not participate in the fenestra ovale. Posteriorly it is in contact with the exoccipitals, the prootics, and anteriorly with the sphenethmoids above, and neopalatines and/or posterior portions of the vomers below. Prechoanal vomer portion lunate, without distinct rami; postchoanal portion acuminate, bearing a small vomerine tooth aggregation separated broadly at the midline. The vomers approach but do not contact one another medially. Neopalatine curving, approaching the medial shelf of the maxilla but not contacting it.

Maxillary arcade and suspensorium. Premaxilla and maxilla bearing teeth. Premaxilla with a narrow medial and broader lateral process, and laterally slanted dorsal process. Maxilla weakly curved, with a narrow lingual shelf. Posteriorly broadly fused to the quadratojugal. Squamosal Y-shaped, otic ramus longer than zygomatic ramus, zygomatic ramus curving anteromedially. Pterygoid Y-shaped, the medial ramus strongly concave posteriorly, the anterior ramus running along the lingual surface of the maxilla, the posterior ramus apparently in synostotic contact with the quadratojugal and squamosal, forming a robust jaw joint.

Mandible. Mentomeckelians small, hourglass shaped. Dentary practically unossified, visible only as a shadow in our micro-CT scan reconstructions. Angulosplenial curved similarly to maxilla; articular facet broadened and inflected slightly ventrally.

Pectoral girdle. No ossified prezonal elements present. Coracoids strongly flared medially, about twice as wide as at the glenoid socket. A weakly mineralized sternum is present. Clavicles thin, strongly curved, more strongly than the anterior surface of the coracoid; starting around the middle of the coracoid. Scapula rather short and broad, with a concave dorsal articulation with the cleithrum. Cleithrum with a well mineralized base and anterior edge, with expanded ossification also at the dorsal end. Suprascapula largely unossified.

Humerus robust, with distinctly raised ventral and lateral crests. Radioulna substantially broadened distally. Ulnare, carpale, carpals 2, 3–5 present. Carpal formula 2-2-3-3, with strongly Y-shaped terminal phalanges on all digits.

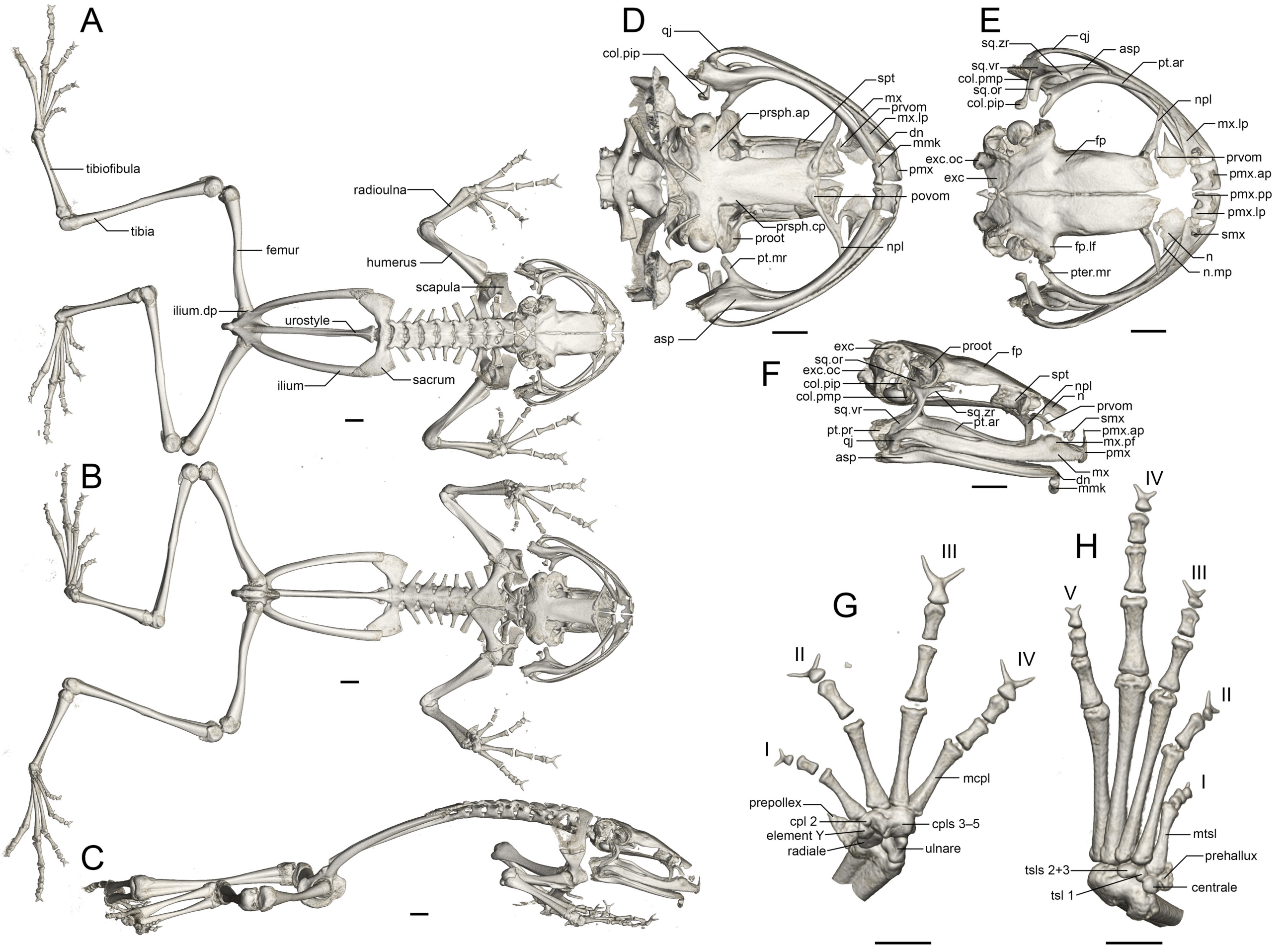

FIGURE 6. Skeletal anatomy of *Platypelis efatra* **sp. nov.** (paratype ZSM 1620/2012), visualized using micro-CT. Showing (A–C) full skeleton in (A) dorsal, (B) ventral, and (C) lateral view; (D–E) skull in (D) ventral, (E) dorsal, and (F) lateral view; and (G) left hand and (H) right foot in ventral view. Abbreviations: asp, angulosplenial; col.pip, pars interna plectri of columella; col.pmp, pars media plectri of columella; cpl(s), carpal(s); dn, dentary; exc, exoccipital; exc.oc, occipital condyle of exoccipital; fp, frontoparietal; fp.lf, lateral flange of frontoparietal; ilium.dp, dorsal prominence of ilium; mmk, mentomeckelian; mcpl, metacarpal; mtsl, metatarsal; mx, maxilla; mx.lp, lingual process of maxilla; mx.pf, pars facialis of maxilla; n, nasal; n.mp, maxillary process of nasal; npl, neopalatine; pmx, premaxilla; pmx.ap, ascending process of premaxilla; pmx.lp, lingual process of premaxilla; pmx.pp, palatine process of premaxilla; povom, post-choanal portion of vomer; proot, prootic; prsph.ap, parasphenoid alary process; prsph.cp, parasphenoid cultriform process; prvom, prevomer; pt.ar, anterior ramus of pterygoid; pt.mr, medial ramus of pterygoid; pt.pr, posterior ramus of pterygoid; qj, quadratojugal; smx, septomaxilla; spt, sphenethmoid; sq.or, otic ramus of squamosal; sq.vr, ventral ramus of squamosal; sq.zr, zygomatic ramus of squamosal. Scale bars = 1 mm.

Vertebral column. Eight procoelous presacral vertebrae, as typical for Cophylinae. Atlas with notably large occipital condyles, almost complete dorsally. Transverse processes rather short and broad, only those of III longer than the centrum is wide; those of II–IV substantially broader than V–VIII. Directions of transverse processes: II, anteroventrolateral; III, posterolateral; IV, posterolateral; V, lateral; VI, slightly anterolateral; VII, more strongly anterolateral; VIII, parallel to VII. No distinct dorsal processes on vertebrae, except a small bulbous anterior projection on II. Sacrum broader than all other vertebrae except III; sacral diapophyses hatchet-shaped, with a straight portion ca 1/3rd of the posterior edge, then bending posteriorly; the distal edge is curved; articulation with urostyle bicondylar. Iliosacral articulation type IIA sensu Emerson (1979); a mineralized extension posterolateral to the diapophysis over the iliac shafts. Urostyle with a dorsal ridge along over half of its length.

Pelvic girdle. Iliac shafts without noticeable dorsal crests. Oblique groove distinct, dorsal prominence very well developed. Pubis and ischium well ossified. Femur slightly sigmoid, with a distinct and low posterior crest. Tibiofibula straight, with a small bulge in the middle. Ulnare-fibulare fused proximally and distally. Mesopodial elements comprising a well developed prehallux, a centrale, and tarsals 1 and 2+3. The toe formula is standard (2-2-3-4-3). The proximal phalange of toe I is very short. Terminal phalanges of all toes Y-shaped, with the arms of the Y as wide or wider than the proximal articulation.

Etymology. The species epithet is a noun in apposition, derived from the Malagasy word efatra = four, making reference to the superficial morphological similarity of the new species to *P. tetra*, whose species epithet also means four in Latinized Greek, referring to the four symmetrical tubercles on its dorsum.

Natural History. Specimens were found in *Pandanus* leaf axils in rainforest. Advertisement calls were not recorded (see below an updated call description for *P. tetra*). In the holotype, and in paratype ZSM 1620/2012, oocytes as visible through the ventral skin are unpigmented and about 2 mm in diameter. Tadpoles unknown.

Distribution. The species is known from (1) its type locality, the Sorata Massif, and from two further sites based on DNA sequences provided by Peloso *et al.* (2016) and Rosa *et al.* (2014), namely (2) Andramanalana (voucher specimen RAX 10391) and (3) Lohanandroranga (voucher specimen RAX 6660 (AMNH A167267)) (see Fig. 2). The elevational range in the Sorata massif is 1339–1558 m a.s.l.

Comparative osteology of *Platypelis tetra*

Based on micro-CT scan of paratype ZSM 42/2011 (originally MRSN A2172) and holotype MRSN A2174 (Fig. 7). Despite scanning artefacts and broken bones (MRSN A2174 has major post-mortem fractures to the ilia, the left femur, the left tibiofibula, the left radioulna, and the proximal phalange of the third toe of the left foot; it also has a developmental error in its presacral vertebra VIII, with the left transverse process developed as a broadened sacrum-like diapophysis), the following features are noted to differ from the specimen of *P. efatra* **sp. nov.** described above (they may constitute further diagnostic differences between the species, but this requires confirmation from analysis of more individuals per species): the zygomatic ramus of the squamosal is shorter than the otic (vs. longer in *P. efatra*) and less curved. Palatal bones are much less ossified and comparison of their anatomy is challenging. Coracoids much less flared medially, being only 1.5 times broader than at the glenoid socket. Presacral vertebrae VII and VIII with transverse processes oriented more laterally. Anterior edge of sacrum almost perpendicular to body axis (vs. angled anteriorly). Urostyle with dorsal crest <50% of its length (vs ≥50%). Dorsal prominence on iliac shafts and oblique groove indistinct (vs. well developed and distinct; although both ilia of the holotype MRSN A2174 are broken at this point).

Advertisement calls of *Platypelis tetra*

Although we were unable to record advertisement calls of the new species for comparison, we here provide an updated description of the advertisement calls assigned to *P. tetra* which we think will be useful for future taxonomic studies of the *P. tetra* complex. The advertisement call recorded on 3 April 2010 at Ambodivoangy (estimated air temperature 26°C) constists of a very short tonal note repeated in long call series (duration of call series up to >30 s) at somewhat irregular intervals (Fig. 8). Each call shows some very slight amplitude modulation with maximum call energy present in the first third of the call's duration. Frequency is distributed in a rather narrow band. Numerical parameters of 53 calls of two males analyzed are as follows: call duration (= note duration) 8–13 ms (10.3 ± 1.3 ms); inter-call interval within call series 227–460 ms (311.7 ± 54.9 ms); dominant frequency 5071–5201 Hz (5149 ± 53 Hz); prevalent bandwidth 4500–5600 Hz. Within regular call series, calls were repeated at an approximate rate of 190–200 calls/minute.

Calls recorded on 5 February 1996 at the type locality in Anjanaharibe Sud Special Reserve (air temperature 18.0–18.5°C) in general character, are in agreement with those reported from Ambodivoangy, but differ by slightly longer call duration and lower dominant frequency (Fig. 8). Numerical parameters of 50 calls of one male analyzed are as follows: call duration (= note duration) 14–20 ms (16.5 ± 1.7 ms); inter-call interval within call series 241–281 ms (261.7 ± 11.1 ms); dominant frequency 3953–4083 Hz (4029 ± 45 Hz); prevalent bandwidth 3500–5000 Hz. Within regular call series, calls were repeated at an approximate rate of 215 calls/minute.

Conservation status of *Platypelis tetra* and *P. efatra*

Platypelis tetra is currently considered as Endangered according to the Red List of the International Union for Conservation of Nature (IUCN SSC Amphibian Specialist Group 2016), based on the assumption that its extent of occurrence (EOO) is 4,759 km^2, spanning a severely fragmented habitat, occurrence in two threat-defined locations,

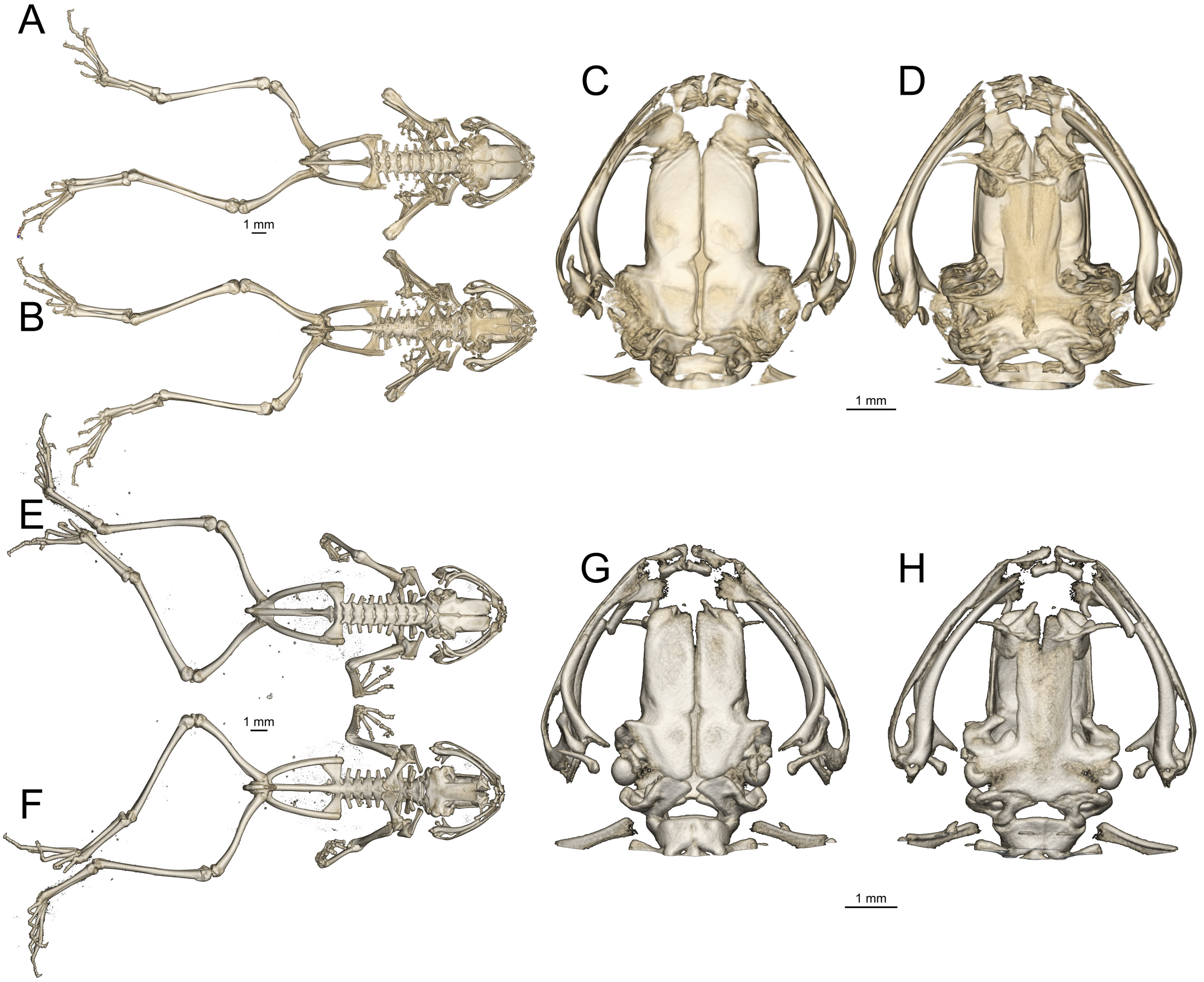

FIGURE 7. Skeletal anatomy of *Platypelis tetra*, based on the holotype MRSN A2174 (A–D) and paratype ZSM 42/2011 (E–H). (A, B, E, F) whole skeleton in (A, E) dorsal and (B, F) ventral view. (C, D, G, H) skull in (C, G) dorsal and (D, H) ventral view. Note that MRSN A2174 moved slightly during scanning, resulting in ghosting artefacts throughout the whole skeleton that make many structures look duplicated or smeared in renders (e.g. neopalatine). Caution should therefore be exercised when interpreting features from this scan.

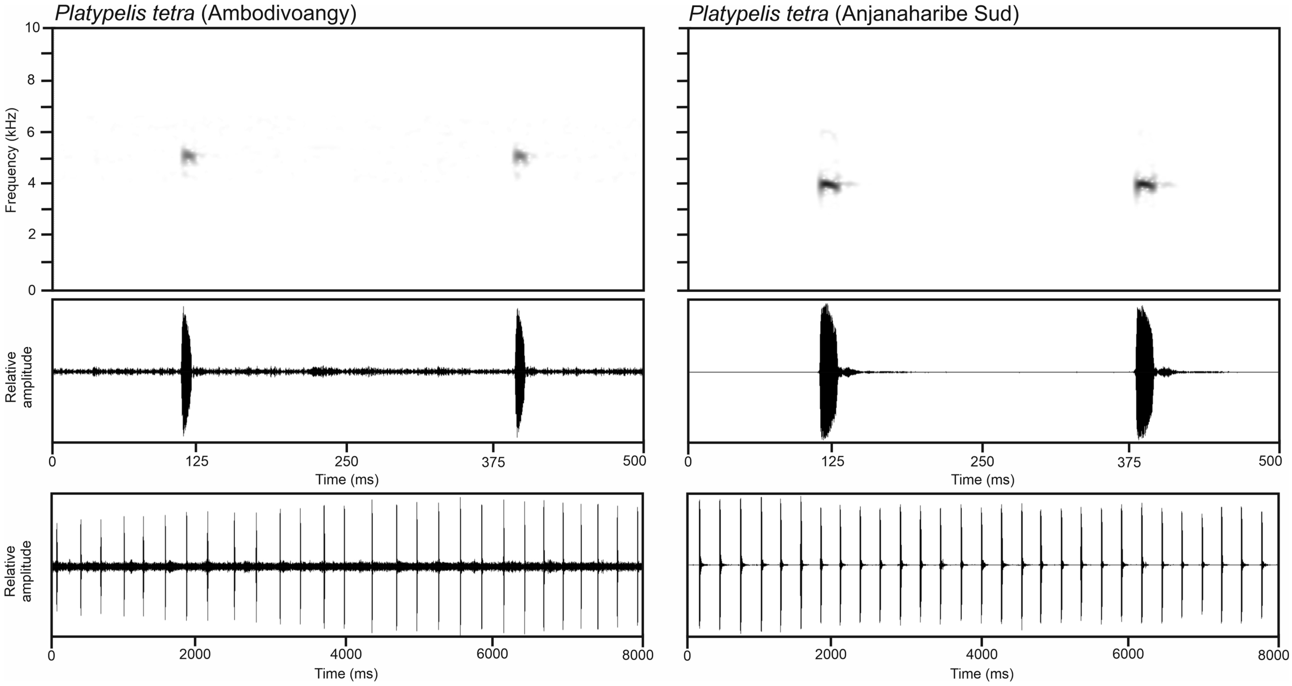

FIGURE 8. Audiospectrograms and corresponding oscillograms of two advertisement calls of *Platypelis tetra* recorded at Ambodivoangy (left; population representing a divergent genetic lineage; see Fig. 1) and at the type locality in Anjanaharibe Sud Special Reserve (right), respectively. Below, oscillograms at 8000 ms time scale showing parts of regular call series. Recordings band-pass filtered at 3500–7000 Hz and 2000–7000 Hz, respectively.

and the ongoing decline in the extent and quality of its habitat in northeastern Madagascar. We here have added a few additional records which, however, did not result in a substantial range extension for the species. Furthermore, our genetic evidence indicates that several of the populations currently assigned to the species may in fact represent other, yet undescribed taxa. Therefore, the current status as Endangered appears to be reasonable. For *P. efatra,* a similar rationale as for *P. tetra* can be applied. The species is currently known from only three threat-defined locations, its EOO is comparable if not smaller than that of *P. tetra*, and there is ongoing decline in the extent and quality of its habitat which in part is outside of effectively protected areas. For a future Red List assessment of this species, a status as Endangered may therefore be appropriate.

Discussion

Although Rakotoarison *et al.* (2023) already published a first DNA sequence from *Platypelis tetra* type material, i.e., from the paratype MRSN A2165, the relationships between the different genetic lineages assigned to the species still remained unclear, perhaps due to the shortness of the obtained sequence (360 bp from the 16S-3' fragment, which did not allow for a reliable phylogenetic placement; see Fig. 1), the lack of sequences from the holotype, and the missing overlap in sequenced 16S fragments of *Platypelis* samples in previous studies. For instance, Gehring *et al.* (2010) published a sequence of the 16S-3' fragment from a sample from Ambodiriana, whereas other studies (e.g., Rakotoarison *et al.* 2020; Rosa *et al.* 2014) sequenced the 16S-5' fragment of the same gene. By providing sequences of the *P. tetra* holotype for both fragments via museomics approaches, and complementing the dataset so that both fragments are included for at least one individual from all populations, we have been able to more reliably reconstruct the mitochondrial genetic relationships between them, and calculate their genetic divergence.

Our data revealed the existence of substantial molecular variation within *P. tetra,* which may be of taxonomic relevance. Specimens from Ambodivoangy (apparently conspecific with specimens from Makira and Ambodiriana) have a dominant frequency of 5071–5201 Hz in their advertisement calls, whereas specimens from the type locality Anjanaharibe Sud have a considerably lower dominant frequency in their calls (3953–4083 Hz) at comparable body sizes. Furthermore the calls of Ambodivoangy specimens also have a shorter note duration of 8–13 ms vs. 14–20 ms, which is a rather static trait unlikely to be influenced by temperature or motivational state of the specimens (Köhler *et al.* 2017). The divergence between these two lineages in the 16S-3' fragment (4.4–5.0%.) is larger than the 3% threshold used by Vieites *et al.* (2009) to characterize candidate species in Malagasy frogs, and these populations therefore may not be conspecific. In this context, it is also relevant that one Makira specimen from 900 m elevation clusters very closely with the holotype from Anjanaharibe-Sud (1250 m a.s.l.), whereas another specimen from low elevation in Makira is placed in the Ambodiriana/Ambodivoangy lineage. The occurrence of the two lineages in close geographical proximity in Makira favors the hypothesis of them representing two distinct species, but in this study, the relevant individuals were not available for morphological examination. Future work, which will further include sequencing of nuclear-encoded gene fragments, will clarify the taxonomic status of these lineages within the *P. tetra* complex.

On the other hand, we deemed the available data as sufficient to conclude that the Sorata lineage, which has previously been provisionally assigned to *P. tetra* (e.g., Rakotoarison *et al.* 2020), represents a distinct species. This is supported by the substantial genetic divergence of >7% in the 16S-3' fragment in concert with subtle morphological differences, but also by its isolated phylogenetic position in the mitochondrial tree, apparently only distantly related to *P. tetra.* By adding a further new species from Sorata, our study contributes to characterizing this Massif as a center of diversity and endemism for *Platypelis* frogs. Combining the data from Rakotoarison *et al.* (2020) and those presented herein, at least five species and one undescribed candidate species of *Platypelis* occur in Sorata: *P. alticola, P. grandis, P. laetus, P. tsaratananaensis, P. efatra*, and *P.* sp. Ca12, of which two (*P. laetus, P.* sp. Ca12) so far are only known from this massif. For *P. efatra*, our tree suggests that also samples from Andramanalana and Lohanandroranga may belong to this species (genetic distance in the 16S-3' fragment: ca. 2%), based on sequences obtained by Peloso *et al.* (2016) and Rosa *et al.* (2014).

One striking aspect of our study is the high morphological similarity between *P. tetra* and *P. efatra*, despite not being each other's closest relatives (in mitochondrial genes). Even osteologically, the two species are rather similar. This confirms that external morphology alone is insufficient for a fully reliable taxonomic resolution in the Cophylinae, and the integration of molecular, bioacoustic and morphological data sets is key to understand their systematics.

Acknowledgments

We are grateful to Angeluc Razafimanantsoa and Théo Rajaofiarison for their assistance in the field, to Gaby Keunecke for help with laboratory work, and to the Malagasy authorities for issuing permits for research, collection, and export of specimens. Hyeun-Ji Lee and Bernhard Ruthensteiner produced some of the analysed micro-CT scans. This work was carried out in the framework of collaboration accords of the Technische Universität Braunschweig and the Zoologische Staatssammlung München with the Université d'Antananarivo, Faculté des Sciences (Mention Zoologie et Biodiversité Animale). Laboratory work at the University of Potsdam was enabled by a collaboration with Michael Hofreiter and financially supported by a grant of the Deutsche Forschungsgemeinschaft (SCHE 2181/1-1) in the framework of the Taxon-Omics priority program (SPP1991). Fieldwork in Sorata was financially supported by the Mohamed bin Zayed Species Conservation Fund (project 11253064) and the BIOPAT initiative (https:// biopat.de).

References

Andreone, F., Fenolio, D.B. & Walvoord, M.E. (2003) Two unknown arboreal frogs (genus *Platypelis*) described from the rainforests of northeastern Madagascar (Microhylidae: Cophylinae). *Current Herpetology*, 22, 91–100. https://doi.org/10.5358/hsj.22.91

Andreone, F., Vences, M., Vieites, D.R., Glaw, F. & Meyer, A. (2005) Recurrent ecological adaptations revealed through a molecular analysis of the secretive cophyline frogs of Madagascar. *Molecular Phylogenetics and Evolution*, 34, 315–322. https://doi.org/10.1016/j.ympev.2004.10.013

Brown, J.L., Sillero, N., Glaw, F., Bora, P., Vieites, D.R. & Vences, M. (2016) Spatial biodiversity patterns of Madagascar's amphibians and reptiles. *PLoS ONE*, 11, e0144076. https://doi.org/10.1371/journal.pone.0144076

Edler, D., Klein, J., Antonelli, A. & Silvestro, D. (2021) raxmlGUI 2.0: A graphical interface and toolkit for phylogenetic analyses using RAxML. *Methods in Ecology and Evolution*, 12, 373–377.
https://doi.org/10.1111/2041-210X.13512

Emerson, S.B. (1979) The ilio-sacral articulation in frogs: form and function. *Biological Journal of the Linnean Society*, 11, 153–168.
https://doi.org/10.1111/j.1095-8312.1979.tb00032.x

Fabrezi, M. & Alberch, P. (1996) The carpal elements of anurans. *Herpetologica*, 52, 188–204.

Fulton, T.L. & Shapiro, B. (2019) Setting up an ancient DNA laboratory. *Methods in Molecular Biology*, 1963, 1–13.
https://doi.org/10.1007/978-1-4939-9176-1_1

Frost, D.R. (2025) *Amphibian Species of the World: An Online Reference*. American Museum of Natural History, New York, USA. Available from: https://amphibiansoftheworld.amnh.org/index.php (accessed 25 June 2025)
https://doi.org/10.5531/db.vz.0001

Gansauge, M.-T., Gerber, T., Glocke, I., Korlević, P., Lippik, L., Nagel, S., Riehl, L.M., Schmidt, A. & Meyer, M. (2017) Single-stranded DNA library preparation from highly degraded DNA using *T4* DNA ligase. *Nucleic Acids Research*, 45, e79.
https://doi.org/10.1093/nar/gkx033

Gehring, P.-S., Ratsoavina, F.M. & Vences, M. (2010) Filling the gaps – amphibian and reptile records from lowland rainforests in eastern Madagascar. *Salamandra*, 46, 214–234.

Glaw, F., Köhler, J. & Vences, M. (2012) A tiny new species of *Platypelis* from the Marojejy National Park in northeastern Madagascar (Amphibia: Microhylidae). *European Journal of Taxonomy*, 9, 1–9.
https://doi.org/10.5852/ejt.2012.9

Glaw, F., Scherz, M.D., Rakotoarison, A., Crottini, A., Raselimanana, A.P., Andreone, F., Köhler, J. & Vences, M. (2020) Genetic variability and partial integrative revision of *Platypelis* frogs (Microhylidae) with red flash marks from eastern Madagascar. *Vertebrate Zoology*, 70, 141–156.

Glaw, F. & Vences, M. (2007) *A Field Guide to the Amphibians and Reptiles of Madagascar*. *3rd Edition.* Vences & Glaw Verlags GbR, Cologne, 496 pp.

IUCN SSC Amphibian Specialist Group. (2016) *Cophyla tetra*. The IUCN Red List of Threatened Species 2016: e.T57962A84179970. Available from: https://doi.org/10.2305/IUCN.UK.2016-1.RLTS.T57962A84179970.en (accessed 16 June 2025)

Katoh, K. & Standley, D.M. (2013) MAFFT multiple sequence alignment software version 7: improvements in performance and usability. *Molecular Biology and Evolution*, 30, 772–780.
https://doi.org/10.1093/molbev/mst010

Köhler, J., Jansen, M., Rodríguez, A., Kok, P.J.R., Toledo, L.F., Emmrich, M., Glaw, F., Haddad, C.F.B., Rödel, M.-O. & Vences, M. (2017) The use of bioacoustics in anuran taxonomy: theory, terminology, methods and recommendations for best practice. *Zootaxa*, 4251 (1), 1–124.
https://doi.org/10.11646/zootaxa.4251.1.1

Kumar, S., Stecher, G. & Tamura, K. (2016) MEGA7: Molecular Evolutionary Genetics Analysis version 7.0 for bigger datasets. *Molecular Biology and Evolution*, 3, 1870–1874.
https://doi.org/10.1093/molbev/msw054

Martin, M. (2011) Cutadapt removes adapter sequences from high-throughput sequencing reads. *EMBnet.journal*, 1, 10–12.
https://doi.org/10.14806/ej.17.1.200

Paijmans, J.L.A., Baleka, S., Henneberger, K., Taron, U.H., Trinks, A., Westbury, M.V. & Barlow, A. (2017) Sequencing single-stranded libraries on the Illumina NextSeq 500 platform. *arXiv*, arXiv:1711.11004.

Palumbi, S.R., Martin, A., Romano, S., McMillan, W.O., Stice, L. & Grabowski, G. (1991) *The simple fool's guide to PCR, Version 2.0*. Privately published, University of Hawaii, Honolulu, 45 pp.

Peloso, P.L.V., Frost, D.R., Richards, S.J., Rodrigues, M.T., Donnellan, S., Matsui, M., Raxworthy, C.J., Biju, S.D., Lemmon, E.M., Lemmon, A.R. & Wheeler, W.C. (2016) The impact of anchored phylogenomics and taxon sampling on phylogenetic inference in narrow-mouthed frogs (Anura, Microhylidae). *Cladistics*, 32, 113–140.
https://doi.org/10.1111/cla.12118

Peloso, P.L.V., Raxworthy, C.J., Wheeler, W.C. & Frost, D.R. (2017) Nomenclatural stability does not justify recognition of paraphyletic taxa: A response to Scherz *et al.* (2016). *Molecular Phylogenetics and Evolution*, 111, 56–64.
https://doi.org/10.1016/j.ympev.2017.03.016

Perl, R.G.B., Nagy, Z.T., Sonet, G., Glaw, F., Wollenberg, K.C. & Vences, M. (2014) DNA barcoding Madagascar's amphibian fauna. *Amphibia-Reptilia*, 35, 197–206.
https://doi.org/10.1163/15685381-00002942

Rakotoarison, A., Crottini, A., Müller, J., Rödel, M.-O., Glaw, F. & Vences, M. (2015) Revision and phylogeny of narrow-mouthed treefrogs (*Cophyla*) from northern Madagascar: integration of molecular, osteological, and bioacoustic data reveals three new species. *Zootaxa*, 3937 (1), 61–89.
https://doi.org/10.11646/zootaxa.3937.1.3

Rakotoarison, A., Glaw, F., Vieites, D.R., Raminosoa, N.R. & Vences, M. (2012) Taxonomy and natural history of arboreal microhylid frogs (*Platypelis*) from the Tsaratanana Massif in northern Madagascar, with description of a new species. *Zootaxa*, 3563 (1), 1–25.

https://doi.org/10.11646/zootaxa3563.1.1

Rakotoarison, A., Scherz, M.D., Bletz, M.C., Razafindraibe, J.H., Glaw, F. & Vences, M. (2019) Description of the lucky *Cophyla* (Microhylidae, Cophylinae), a new arboreal frog from Marojejy National Park in north-eastern Madagascar. *Zootaxa*, 4651 (2), 271–288.
https://doi.org/10.11646/zootaxa.4651.2.4

Rakotoarison, A., Scherz, M.D., Köhler, J., Ratsoavina, F.M., Hawlitschek, O., Megson, S., Vences, M. & Glaw, F. (2020) Frogs of the genus *Platypelis* from the Sorata massif in northern Madagascar: description of a new species and reports of range extensions. *Zoosystematics and Evolution*, 96, 263–274.
https://doi.org/10.3897/zse.96.47088

Rakotoarison, A., Scherz, M.D., Mullin, K.E., Crottini, A., Petzold, A., Ranjanaharisoa, F.A., Maheritafika, H.M.R., Rafanoharana, J.M., Raherinjatovo, H., Andreone, F., Glaw, F. & Vences, M. (2023) Gray versus yellow ventral coloration: Identity, distribution, color polymorphism and molecular relationships of the microhylid frog *Platypelis mavomavo* Andreone, Fenolio & Walvoord, 2003. *Zootaxa*, 2352 (2), 221–234.
https://doi.org/10.11646/zootaxa.5352.2.4

Rohland, N., Siedel, H. & Hofreiter, M. (2004) Nondestructive DNA extraction method for mitochondrial DNA analyses of museum specimens. *Biotechniques*, 36, 814–821.
https://doi.org/10.2144/04365ST05

Rosa, G., Crottini, A., Noël, J., Rabibisoa, N., Raxworthy, C.J. & Andreone, F. (2014) A new phytotelmic species of *Platypelis* (Microhylidae: Cophylinae) from the Betampona Reserve, eastern Madagascar. *Salamandra*, 50 (4), 201–214.

Scherz, M.D., Köhler, J., Vences, M. & Glaw, F. (2019) A new yellow-toed *Platypelis* species (Anura, Microhylidae, Cophylinae) from the Maroantsetra region, northeastern Madagascar. *Evolutionary Systematics*, 3, 75–83.
https://doi.org/10.3897/evolsyst.3.33417

Scherz, M.D., Vences, M., Rakotoarison, A., Andreone, F., Köhler, J., Glaw, F. & Crottini, A. (2016) Reconciling molecular phylogeny, morphological divergence and classification of Madagascan narrow-mouthed frogs (Amphibia: Microhylidae). *Molecular Phylogenetics and Evolution*, 100, 372–381.
https://doi.org/10.1016/j.ympev.2016.04.019

Scherz, M.D., Vences, M., Rakotoarison, A., Andreone, F., Köhler, J., Glaw, F. & Crottini, A. (2017a) Lumping or splitting in the Cophylinae (Anura: Microhylidae) and the need for a parsimony of taxonomic changes: a response to Peloso *et al.* (2017). *Salamandra*, 53, 479–483.

Scherz, M.D., Hawlitschek, O., Andreone, F., Rakotoarison, A., Vences, M. & Glaw, F. (2017b) A review of the taxonomy and osteology of the *Rhombophryne serratopalpebrosa* species group (Anura: Microhylidae) from Madagascar, with comments on the value of volume rendering of micro-CT data to taxonomists. *Zootaxa*, 4273 (3), 301–340.
https://doi.org/10.11646/zootaxa.4273.3.1

Scherz, M.D., Crottini, A. & Rakotoarison, A. (2022) Microhylidae: Cophylinae, Microhylid frogs. *In*: Goodman, S.M. (Ed.), *The New Natural History of Madagascar*. *Vol. 2.* Princeton University Press, Princeton, New Jersey, pp. 1382–1390.
https://doi.org/10.2307/j.ctv2ks6tbb.195

Stamatakis, A. (2014) RAxML version 8: A tool for phylogenetic analysis ad post-analysis of large phylogenies. *Bioinformatics*, 30, 1312–1313.
https://doi.org/10.1093/bioinformatics/btu033

Straube, N., Lyra, M.L., Paijmans, J.L.A., Preick, M., Basler, N., Penner, J., Rödel, M.-O., Westbury, M.V., Haddad, C.F., Barlow, A. & Hofreiter, M. (2021) Successful application of ancient DNA extraction and library construction protocols to museum wet collection specimens. *Molecular Ecology Resources*, 21, 2299–2315.
https://doi.org/10.1111/1755-0998.13433

Trueb, L. (1968) Cranial osteology of the hylid frog, *Smilisca baudini*. *University of Kansas Publications, Museum of Natural History*, 18, 11–35.

Trueb, L. (1973) Bones, frogs, and evolution. *In*: Vial, J.L. (Ed.), *Evolutionary Biology of the Anurans: Contemporary Research on Major Problems*. University of Missouri Press, Columbia, Missouri, pp. 65–132.

Van der Meijden, A., Vences, M., Hoegg, S., Boistel, R., Channing, A. & Meyer, A. (2007) Nuclear gene phylogeny of narrow-mouthed toads (Family: Microhylidae) and a discussion of competing hypotheses concerning their biogeographical origins. *Molecular Phylogenetics and Evolution*, 44, 1017–1030.
https://doi.org/10.1016/j.ympev.2007.02.008

Vences, M., Glaw, F. & Márquez, R. (2006) *The Calls of the Frogs of Madagascar*. Alosa-Fonozoo, Barcelona, 44 pp.

Vences, M., Kosuch, J., Glaw, F., Böhme, W. & Veith, M. (2003) Molecular phylogeny of hyperoliid treefrogs: biogeographic origin of Malagasy and Seychellean taxa and re-analysis of familial paraphyly. *Journal of Zoological Systematics and Evolutionary Research*, 41, 205–215.
https://doi.org/10.1046/j.1439-0469.2003.00205.x

Vences, M., Miralles, A., Brouillet, S., Ducasse, J., Fedosov, A., Kharchev, V., Kostadinov, I., Kumari, S., Patmanidis, S., Scherz, M.D., Puillandre, N. & Renner, S.S. (2021) iTaxoTools 0.1: Kickstarting a specimen-based software toolkit for taxonomists. *Megataxa*, 6 (2), 77–92.
https://doi.org/10.11646/megataxa.6.2.1

Vences, M., Patmanidis, S., Kharchev, V. & Renner, S.S. (2022) Concatenator, a user-friendly program to concatenate DNA sequences, implementing graphical user interfaces for MAFFT and FastTree. *Bioinformatics Advances*, 2, vbac050. https://doi.org/10.1093/bioadv/vbac050

Vieites, D.R., Wollenberg, K.C., Andreone, F., Köhler, J., Glaw, F. & Vences, M. (2009) Vast underestimation of Madagascar's biodiversity evidenced by an integrative amphibian inventory. *Proceedings of the National Academy of Sciences of the U.S.A.*, 106, 8267–8272. https://doi.org/10.1073/pnas.0810821106

Wollenberg, K.C., Vieites, D.R., van der Meijden, A., Glaw, F., Cannatella, D.C. & Vences, M. (2008) Patterns of endemism and species richness in Malagasy cophyline frogs support a key role of mountainous areas for speciation. *Evolution*, 62, 1890–1907. https://doi.org/10.1111/j.1558-5646.2008.00420.x